Solution Structure of the Immunodominant Region of Protein G of Bovine Respiratory Syncytial Virus[†,‡]

Jurgen F. Doreleijers,[§] Johannes P. M. Langedijk,[||] Karl Hård,[§,⊥] Rolf Boelens,[§] Johan A. C. Rullmann,[§] Wim M. Schaaper,[#] Jan T. van Oirschot,[||] and Robert Kaptein*[,§]

Bijvoet Center for Biomolecular Research, Utrecht University, Padualaan 8, 3584 CH Utrecht, The Netherlands, and Departments of Mammalian Virology and Molecular Recognition, Institute for Animal Science and Health, P.O. Box 65, 8200 AB Lelystad, The Netherlands

Received August 26, 1996; Revised Manuscript Received October 7, 1996[⊗]

ABSTRACT: The three-dimensional solution structure of the immunodominant central conserved region of the attachment protein G (BRSV-G) of bovine respiratory syncytial virus has been determined by nuclear magnetic resonance (NMR) spectroscopy. In the 32-residue peptide studied, 19 residues form a small rigid core composed of two short helices, connected by a type I′ turn, and linked by two disulfide bridges. This unique fold is among the smallest stable tertiary structures known and could therefore serve as an ideal building block for the design of *de novo* proteins and as a test case for modeling studies. A characteristic hydrophobic pocket, lined by conserved residues, lies at the surface of the peptide and may play a role in receptor binding. This work provides a structural basis for further peptide vaccine development against the severe diseases associated with the respiratory syncytial viruses in both cattle and man.

Bovine respiratory syncytial virus (BRSV)[1] accounts for a high proportion of morbidity and mortality in cattle (Stott & Taylor, 1985; Baker et al., 1986), resulting in considerable economic losses. Furthermore, human RSV (HRSV) is a major cause of serious respiratory infections including bronchiolitis and pneumonia in infants and young children: these conditions are responsible for almost 100 000 hospitalizations yearly in the USA alone (Heilman, 1990). The development of efficacious vaccines against HRSV infections has a very high priority according to the World Health Organization (1995) and has lately received much attention (Hall, 1994; McIntosh & Chanock, 1990).

Respiratory syncytial virus carries two glycoproteins on its surface: the fusion protein F and the attachment protein G. The latter is an integral membrane protein and is functionally distinct from other viral attachment proteins. The focus of the present study is the small conserved hydrophobic domain (Figure 1) that is located in the ectodomain and is presumably flanked in the intact protein G by two extended mucin-like regions (Langedijk et al., 1996b). This domain contains four conserved cysteines which form two disulfide bridges. Peptides based on this domain were found to be immunodominant in protein G of both HRSV (Norrby et al., 1987; Åkerlind-Stopner et al., 1990) and BRSV (Langedijk et al., 1996b); they can be used as antigens in highly specific and sensitive immunoassays (Langedijk et al., 1996a) and have conferred protection against HRSV challenge in mice (Trudel et al., 1991).

We have studied a 32-residue synthetic peptide representing the conserved central region of protein G of BRSV using two-dimensional (2D) NMR, distance geometry (DG), and restrained molecular dynamics (RMD).

MATERIALS AND METHODS

Peptide Preparation. The synthesis of the peptide corresponding to the central hydrophobic region of BRSV-G, strain 391−2 (Lerch et al., 1990) was performed according to standard procedures using Fmoc chemistry (Fields et al. 1991). Disulfides were formed under mild oxidative conditions. The peptide was purified by HPLC and FPLC as described in Langedijk et al. (1996b).

NMR Spectroscopy. For this study 2D nuclear Overhauser effect spectroscopy (NOESY; 25, 50, 100, and 200 ms) (Jeener et al., 1979), total correlation spectroscopy (TOCSY; 30 and 70 ms) (Braunschweiler & Ernst, 1983), double-quantum-filtered correlation spectroscopy (DQF-COSY) (Rance et al., 1983), and ^{13}C natural abundance heteronuclear single-quantum coherence spectroscopy (HSQC) (Bodenhausen & Ruben, 1980) experiments were recorded on Varian Unity+ 750 MHz and Bruker AMX 500 MHz spectrometers at 285 K. The sample was obtained with 6.1 mM peptide

[†] The 750 MHz NMR spectra were recorded at the SON NMR Large Scale Facility (Utrecht), which is supported by the Large Scale Facility Program of the European Union.

[‡] Coordinates and experimental NMR data of the C-terminal domain of the peptide have been deposited in the Brookhaven Protein Data Bank (filename 1BRV).

* To whom correspondence should be addressed: Department of NMR Spectroscopy, Utrecht University, Padualaan 8, 3584 CH Utrecht, The Netherlands. Telephone: +31-30-2532652. Fax: +31-30-2537623.

[§] Utrecht University.

[||] Department of Mammalian Virology, Institute for Animal Science and Health.

[⊥] Present address: Leiden Institute of Chemistry, Leiden University, P.O. Box 9502, 2300 RA Leiden, The Netherlands.

[#] Department of Molecular Recognition, Institute of Animal Science and Health.

[⊗] Abstract published in *Advance ACS Abstracts,* November 1, 1996.

[1] Abbreviations: RSV, respiratory syncytial virus; BRSV, bovine RSV; HRSV, human RSV; BRSV-G, protein G of BRSV; 2D, two dimensional; NMR, nuclear magnetic resonance; ppm, parts per million; rms, root mean square; DG, distance geometry; RMD, restrained molecular dynamics; NOE, nuclear Overhauser effect; DQF-COSY, double-quantum-filtered correlation spectroscopy; TOCSY, 2D total correlation spectroscopy; NOESY, 2D NOE spectroscopy; HSQC, heteronuclear single-quantum coherence spectroscopy; PDB, Protein Data Bank of Brookhaven National Laboratory.

S0006-2960(96)02162-9 CCC: $12.00

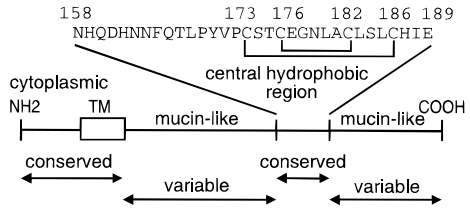

FIGURE 1: Modular arrangement of BRSV-G and amino acid sequence of the central conserved region studied. The box indicates the transmembrane region (TM). The disulfide-bridged cysteines are connected by lines. The arrows highlight the relatively conserved parts of the protein.

in a 95:5 $^1H_2O/^2H_2O$ mixture or 99.9% ^2H_2O containing trace amounts of TSP and NaN_3 at pH 4.6. The data were zero-filled and processed by apodization with a phase-shifted sine-square window function in both dimensions before Fourier transformation and baseline correction. The final size of the matrices was 2K × 1K real points (TOCSY, NOESY, and HSQC) or 4K × 1K real points (DQF-COSY). Spectra were processed with our in-house NMR program package TRITON and analyzed with the program REGINE on a Silicon Graphics Indy workstation.

Experimental Restraints. The NOE volumes obtained from the 100 ms 750 MHz NOESY spectrum were translated into upper distance bounds. Calibration was performed using the sequential contacts $d_{\alpha N}$ set to 3.5 Å in the an α-helical region. Lower distance bounds were in all cases taken as the sum of the van der Waals radii of two hydrogen atoms (1.8 Å). Pseudoatom corrections were added for nonstereospecifically assigned prochiral methylene groups (0.9 Å), methyl groups (0.3 Å), and Leu and Val dimethyl groups (1.8 Å). All NOE restraints were increased by 10% to reflect an experimental uncertainty. An additional 20% was added to restraints involving methyl groups to account for the multiplicity of these spins.

The distance restraints were supplemented with φ and χ_1 dihedral restraints. φ dihedral restraints ($-120 \pm 20°$) were introduced for residues in an extended conformation on the basis of the coupling constant $^3J_{\alpha N} > 9$ Hz. χ_1 dihedrals were found together with the stereospecific assignment of prochiral β protons from a combined analysis of $^3J_{\alpha\beta}$ coupling constants, obtained from DQF-COSY experiments, and NOEs from short mixing time NOESY experiments (Wagner et al., 1987). Magnetization transfer from NH and αH to βH in a short mixing time TOCSY experiment is used together with the $^3J_{\alpha\beta}$ observed in the DQF-COSY experiment (Clore et al., 1991). Although some slowly exchanging amides were found (data not shown), no restraints enforcing hydrogen bonds were used.

Structure Calculation. The three-dimensional structure of the segment was calculated with DG and subsequently optimized by RMD based on NOE distance restraints, φ and χ_1 dihedral angle restraints, and explicit disulfide bonds. Neither hydrogen bonds nor electrostatics were included in the calculations. Additional restraints were included to maintain chirality and peptide bond planarity. The force constants for distance and dihedral restraints were 40 kcal·mol^{-1}·Å^{-2} and 30 kcal·mol^{-1}·rad^{-2}, respectively.

Structures were calculated with the DGII program (Havel, 1991) within the InsightII NMRchitect package (Biosym Technologies, San Diego, CA). A subsequent 10 ps RMD (Kaptein et al., 1985) at 300 K with the Discover program (Biosym Technologies) sampled and further optimized the

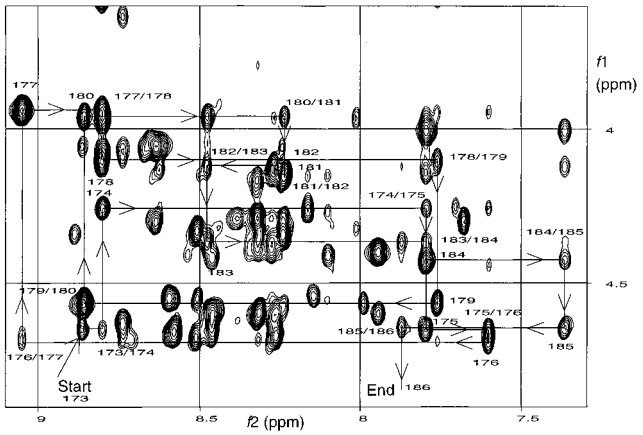

FIGURE 2: Fingerprint region of the 100 ms NOESY spectrum of the immunodominant region of BRSV-G recorded at 285 K and 750 MHz. From the first to the last cysteine (Cys173−Cys186, indicated by start and end) the sequential walk (connecting intra- and interresidual connectivities) is drawn.

local geometry. The final set of structures was selected only on the basis of the error function in the DG calculation. The coordinates of the structures and experimental restraints have been deposited in the Protein Data Bank of Brookhaven National Laboratory (PDB, accession code 1BRV).

RESULTS AND DISCUSSION

Resonance Assignment. The complete sequence-specific assignment (Wüthrich, 1985) was obtained with the use of 2D TOCSY, NOESY, and DQF-COSY recorded at 500 and 750 MHz. Part of the 100 ms NOESY, used to extract the NOE distance restraints, is shown in Figure 2, illustrating the sequential assignment. The ^1H and ^{13}C chemical shifts of the peptide are available as Supporting Information.

Proline Isomerization. The peptide bond between Leu168 and Pro169, located in the flexible N-terminus as discussed below, was found to be in a *cis*:*trans* (16%:84%) equilibrium. This was evidenced by a secondary chemical shift (deviation from the random coil value) of Pro169 Cγ of 3.0 ppm upfield in the *cis*-amide isomer relative to the *trans*-amide isomer (Grathwohl & Wüthrich, 1976). For the minor species a characteristic strong NOE between the α protons of Leu168 and Pro169 confirmed the *cis* peptide bond between the two residues. In the main species, Pro169 and Pro172 show strong NOEs between their δ protons and the α protons of the preceding residue, and regular secondary chemical shifts for the γ carbons of the prolines, which can only be observed when *trans* peptide bonds are present. Isomerization of the peptide bond between Val171 and Pro172 was not observed. The minor *cis*-Pro169 species was partly assigned (data not shown) and excluded from subsequent analysis.

Disulfide Bridge Connectivity. The disulfide bridges were unambiguously assigned as Cys173−Cys186 (outer bridge) and Cys176−Cys182 (inner bridge) on the basis of long-range NOEs between the specific cysteines and surrounding residues. Both of the other possible disulfide bridge connectivities (173−176, 182−186 and 173−182, 176−186) produce structures with severe discrepancies with the NMR data (data not shown). Analysis of proteolytic digestion products and affinity measurements with peptide variants (Langedijk et al., 1996b), in which different disulfide connections were established, is in accordance with the NMR assignment.

Table 1: Structural Statistics for the Immunodominant Region of BRSV-G[a]

Rms Deviation from Average Structure (Å)[b]	
backbone atoms (N, Cα, C′)	0.18 ± 0.05
all heavy atoms	0.56 ± 0.09
Average Distance Restraint Violations	
violation (Å)	0.09 ± 0.07
max violation (Å)	0.34 ± 0.01
no. of violations ≥0.2 Å per model	5 ± 1
Ramachandran and Contact Statistics	
% of residues with ϕ/ψ in	
most favored regions	91.1
additional allowed regions	8.9
disallowed regions	0.0
av no. of bad noncovalent contacts	0.2

Dihedral Angle Comparison (deg)

	BRSV-G region	Engh & Huber[c]
χ_1^{g-}	71.0 ± 9.7	64.1 ± 15.7
χ_1^{trans}	194.4 ± 7.4	183.6 ± 16.8
χ_1^{g+}	−67.6 ± 20.3	−66.7± 15.0
χ_2	176.0 ± 7.7	177.4 ± 18.5
ϕ-helix	−67.8 ± 13.7	−65.3 ± 11.9
ψ-helix	−33.6 ± 11.3	−39.4 ± 11.3
ω	175.9 ± 6.5	180.0 ± 5.8
Cα chirality	33.5 ± 2.8	33.9 ± 3.5

[a] The structural statistics were calculated with PROCHECK-NMR (Laskowski et al., 1996), a variant of the PROCHECK program (Laskowski et al., 1993). [b] Residues Pro172 to Cys186. [c] The comparison of the dihedral angles is made with values found from Engh and Huber (1991).

Three-Dimensional Structure. No long-range and very few medium-range NOE contacts were found for the N-terminal region (Asp158−Tyr170), which was therefore excluded in the structure calculations. Furthermore, the resonances of spins in this region resemble those in a random coil conformation, which is another indication that the N-terminus is flexible.

For the remaining 19 residues we obtained 264 nonredundant NOE distance restraints (approximately 14 restraints per residue) including 76 intraresidual, 83 sequential, 72 medium-range ($|i - j| < 5$), and 33 long-range NOEs. In addition, we used two φ (for residues 187 and 188) and nine χ_1 dihedral restraints (for residues 173, 174, 176, 179, 180, 182, 183, 186, and 187). The average line width (approximately 8 Hz at 285 K) did not allow the accurate determination of the small $^3J_{\alpha N}$ couplings present in residues with a helical conformation, where $^3J_{\alpha N} \ll$ line width, and these were therefore not included. The nine χ_1 dihedrals were found together with the stereospecific assignment of eight prochiral β proton pairs.

From a total of 50 calculated structures we selected 48 structures (96%), shown in Figure 3A. The backbone atoms (N, Cα, C′) from residues Pro172 to Cys186 of these structures superimpose on the average structure with a root-mean-square (rms) difference of 0.18 ± 0.07 Å. The structural statistics of the 48 selected structures listed in Table 1 show that there is good accordance with the experimental data (Laskowski et al., 1996) and stereochemical quantities as determined from high-resolution structures (Engh & Huber, 1991).

The structured region, as determined with the DSSP program (Kabsch & Sander, 1983), begins with one turn of α-helix (Cys173−Cys176) which runs antiparallel to the $1^1/_2$ α-helical turns formed by Leu180−Leu185. In 15 models (31%) the first helix was classified as a 3_{10}-helix. The inner disulfide bridge (176−182) has a left-handed conformation ($\chi_3 = -56 \pm 1°$) but the outer disulfide bridge (173−186) is less well defined and occurs mostly in a left-handed ($\chi_3 = -72 \pm 2°$; 69%) but also in a right-handed conformation ($\chi_3 = 64 \pm 2°$; 31%). Most models for which the first helix was classified as a 3_{10}-helix were also found to have the outer disulfide bridge in a right-handed conformation. The right- and left-handed conformations of the disulfide bridge may be in rapid exchange since no specific line broadening was observed in the proximity of this moiety.

The two helices are furthermore linked by a reverse type I turn (Cys176−Asn179). Asparagine 179 is involved in three hydrogen bonds (Figure 3B): its backbone amide with the carbonyl of Cys176 in the type I′ turn capping the C-terminus of the first helix, its backbone oxygen with the amide of Leu183 in the second helix, and its side-chain oxygen with the amide of Cys182 capping the N-terminus of the second helix. The secondary chemical shift of the α carbon (Spera & Bax, 1991) of this asparagine (1.7 ppm upfield, as shown in Figure 4) is reminiscent of a N-cap residue, mainly due to the large value of its ψ angle (Gronenborn & Clore, 1994). Also the secondary chemical shifts of other α carbons demonstrate close correspondence with the secondary chemical shifts expected for the observed conformations (Figure 4). Asparagine is frequently found as a N-cap (Richardson & Richardson, 1988). Only aspartate shares this ability and is found at the same position in protein G of ovine RSV. Glycine frequently occurs at the C-capping position (Richardson & Richardson, 1988), as in protein G of HRSV strain 18537, a subgroup B virus (Wertz et al., 1985). In BRSV-G, Gly178 is located one residue away from that position and serves to relax the turn by its larger allowed conformational space.

The overall shape of the two linked helices (Cys173−Cys186) is that of a 9 Å thick disk with a diameter of about 20 Å. On the front face the side-chain amide of Asn179 extends into solution. Most striking is a hydrophobic pocket with suitable dimensions (approximately cubic with 4 Å edges) to bind a small ligand or amino acid side chain. The pocket is lined only by the conserved residues Cys176 and Cys182 (top), Leu185 and Cys186 (right), Val171 and Pro172 (bottom), and Cys173 (left) shown in Figure 3C. The sulfur atom of Cys182 has a large surface accessibility, but Cys176 was found to be the most important residue for specific binding of a BRSV-G specific monoclonal antibody mapped to residues 176−185 (CEGNLACLSL) (Langedijk et al., 1996b). The backbone oxygen atom of Cys182 is the only exposed hydrophilic atom in the pocket and is hydrogen bonded with the amide proton of Cys186. The residues forming the pocket are more conserved in the different RSV than the residues between the inner disulfide bridge. This suggests that the RSV-G receptor will have a general hydrophobic interaction with the conserved pocket with a receptor site that is common to all RSV-G receptors. Binding with the rest of the surface, which is formed for a large part by nonconserved residues, may be specific for each RSV type.

Homology. The overall fold presented here is unique, and no homology was found with other protein fragments in the structural databases of DALI (Holm & Sander, 1993) and WHAT IF (Vriend, 1990). The loop between the inner

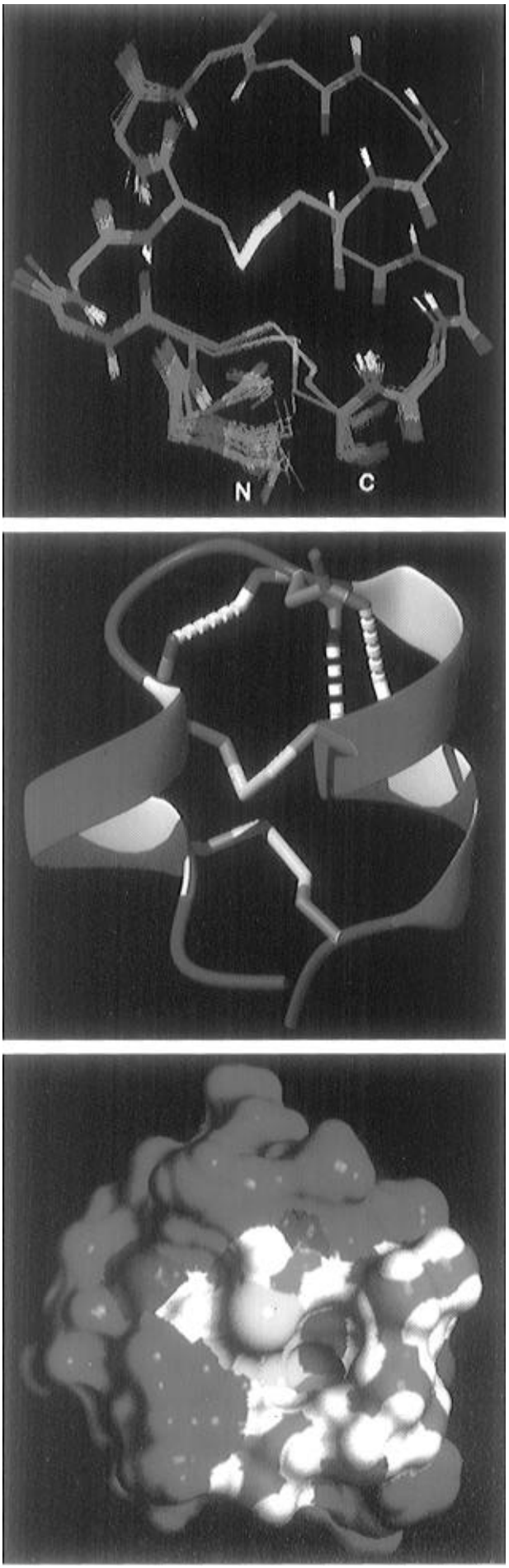

disulfide bridge, however, is quite general. In a search for structural similarities, performed with the WHAT IF program, more than ten fragments (seven residues long) were found to have rms differences below 1 Å with residues Cys176−Cys182 of BRSV-G. In this search no requirement was set on the terminal residues to be cysteines or a cystine.

Cystine Noose. These disulfide-constrained, surface-exposed loops, like the one found in BRSV-G (Cys176−Cys182), have recently been identified as a structural motif termed "cystine noose" that may be important in receptor-binding specificity (Lapthorn, 1995). Cystine nooses, however, have not previously been found to be located between two helices. The sweet-tasting protein thaumatin I (PDB, accession code 1THV) has the smallest rms difference (1 Å; Cys71−Cys77) with the BRSV-G noose when the inner disulfide connection is also taken into account. It differs from the BRSV-G noose by having deviating dihedrals, no flanking helices, and no outer disulfide bridge. Another interesting homology exists with the immunodominant domain of HIV-1 gp41 transmembrane protein (Oldstone et al., 1991), which shares both a local sequence and a structural similarity with the BRSV-G noose. Although no detailed structure has been reported for HIV-1 gp41, the inner disulfide bridge and a type I′ turn were found at the same place as in the BRSV-G noose.

The BRSV-G fragment as a whole is unusually compact and rigid for such a small peptide. The ease at which it is able to fold and form the correct disulfide bridges *in vitro* (Langedijk et al., 1996b), in combination with its size, makes it an ideal building block for the design of *de novo* proteins (Struthers et al., 1995).

A structural consequence of the hairpin topology of the present structure would be the antiparallel alignment of both mucin-like regions (Langedijk et al., 1996b) exposing the immunodominant region for interaction with the receptor.

CONCLUSIONS

The solution structure of the immunodominant region of protein G of BRSV is composed of two short helices connected by two disulfide bridges forming a compact assembly. A cystine noose, exposing residues to the surface, was found which may be important in receptor-binding specificity. Knowledge of the surface of BRSV-G will facilitate the search for the protein G receptor itself. The conserved pocket may be useful for the design of drugs against RSV infections.

FIGURE 3: Solution structure of the immunodominant region of BRSV-G. (A, top) Backbone traces and disulfide bridges of 48 superimposed structures. The termini are labeled N and C. Atoms are colored as follows: hydrogen (white), carbon (green), nitrogen (blue), oxygen (red), and sulfur (yellow). (B, middle) Model of the best structure (closest to the ensemble average) highlighting the doubly disulfide-bridged helices (blue) and the hydrogen-bonding network of Asn179 (white). The atoms of Asn179 and their hydrogen-bonded partners as well as the atoms forming the disulfide bridge are drawn as sticks. Residues having a nonhelical conformation are colored red. (C, bottom) Connolly surface featuring the hydrophobic pocket lined by conserved residues, which are colored by atom. The surface was calculated with a 1.3 Å radius probe to mimic a water molecule. The displayed residues are Val171−Cys186, His187, and Glu189 in (A), (B), and (C) respectively. Almost the same orientation for the molecules is used in each of these figures.

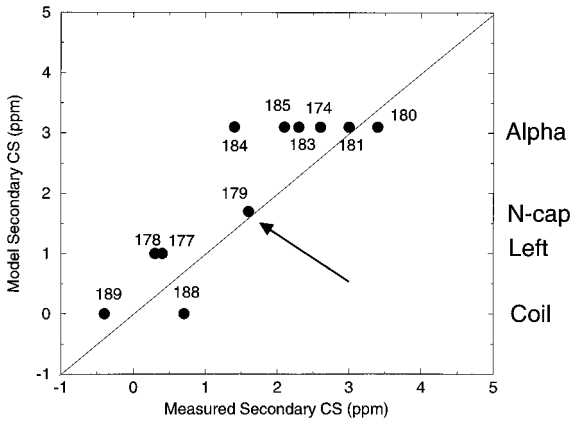

FIGURE 4: Correlation plot between the measured secondary chemical shifts of $^{13}C\alpha$ of residues Ser174−Glu189 and the standard secondary chemical shifts expected for these residues in the conformation they have in the calculated set of structures. The secondary chemical shift of Asn179 is indicated by an arrow. Note that residues 175, 176, 182, 186, and 187 are not shown because either their Cα resonance could not be assigned or the coil chemical shift was not available. The secondary chemical shifts 0, 1.0, and 3.1 for residues in a coil, left-handed α-helix, or right-handed α-helix conformation, respectively, are taken from Spera and Bax (1991).

ACKNOWLEDGMENT

We thank John Martin for carefully reading the manuscript and Gert Vriend for noting some of the unique features of the structure.

SUPPORTING INFORMATION AVAILABLE

^{1}H and ^{13}C chemical shifts of the immunodominant region of BRSV-G (2 pages). Ordering information is given on any current masthead page.

REFERENCES

Åkerlind-Stopner, B., Utter, G., Mufson, M. A., Orvell, C., Lerner, R. A., & Norrby, E. (1990) *J. Virol. 64*, 5143−5148.
Baker, J. C., Werdin, R. E., Ames, T. R., Markham, R. J. F., & Larson, V. L. (1986*) J. Am. Vet. Med. Assoc. 189*, 66−70.
Bodenhausen, G., & Ruben, D. J. (1980) *Chem. Phys. Lett. 69*, 185−189.
Braunschweiler, L., & Ernst, R. R. (1983) *J. Magn. Reson. 53*, 521−528.
Clore, G. M., Bax, A., & Gronenborn, A. M. (1991) *J. Biomol. NMR 1*, 13−22.
Collins, P. L., & Mottet, G. (1992) *J. Gen. Virol. 73* (Part 4), 849−863.
Engh, R. A., & Huber, R. (1991) *Acta Crystallogr. A47*, 392−400.
Fields, C. G., Lloyd, D. H., MacDonald, R. L., Otteson, K. M., & Noble, R. L. (1991*) Peptide Res. 4*, 95−101.
Grathwohl, C., & Wüthrich, K. (1976) *Biopolymers 15*, 2025−2041.
Gronenborn, A. M., & Clore, G. M. (1994) *J. Biomol. NMR 4*, 455−458.
Hall, C. B. (1994) *Science 265*, 1393−1394.
Havel, T. F. (1991) *Prog. Biophys. Mol. Biol. 56*, 43−78.
Heilman, C. A. (1990) *J. Infect. Dis. 161*, 402−406.
Holm, L., & Sander, C. (1993) *J. Mol. Biol. 233*, 123−138.
IUPAC−IUB Commission on Biochemical Nomenclature (1970) *Biochemistry 9*, 3471−3479.
Jeener, J., Meier, B. H., Bachmann, P., & Ernst, R. R. (1979) *J. Chem. Phys. 71*, 4546−4553.
Kabsch, W., & Sander, C. (1983) *Biopolymers 22*, 2577−2637.
Kaptein, R., Zuiderweg, E. R. P., Scheek, R. M., Boelens, R., & van Gunsteren, W. F. (1985) *J. Mol. Biol. 182*, 179−182.
Kuroda, Y. (1995) *Protein Eng. 8*, 97−101.
Langedijk, J. P. M., Middel, W. G. J., Schaaper, W. M. M., Meloen, R. H., Kramps, J. A., Brandenburg, A. H., & van Oirschot, J. T. (1996a) *J. Immunol. Methods 193*, 157−166.
Langedijk, J. P. M., Schaaper, W. M. M., Meloen, R. H., & van Oirschot, J. T. (1996b) *J. Gen. Virol. 77*, 1249−1257.
Lapthorn, A. J., Janes, R. W., Isaacs, N. W., & Wallace, B. A. (1995) *Nat. Struct. Biol. 2*, 266−268.
Laskowski, R. A., MacArthur, M. W., Moss, D. S., & Thornton, J. M. (1993) *J. Appl. Crystallogr. 26*, 283−291.
Laskowski, R. A., Rullmann, J. A. C., MacArthur, M. W., Kaptein, R., & Thornton, J. M. (1996) *J. Biomol. NMR* (in press).
Lerch, R. A., Anderson, K., & Wertz, G. W. (1990) *J. Virol. 64*, 5559−5569.
McIntosh K. M., & Chanock R. M. (1990) in *Virology* (Fields, B. N., Ed.) pp 1045−1072, Raven Press, New York, NY.
Norrby, E., Mufson, M. A., Alexander, H., Houghten, & Lerner, R. A. (1987) *Proc. Natl. Acad. Sci. U.S.A. 84*, 6572−6575.
Oldstone, M. B. A., Tishon, A., Lewicki, H., Dyson, H. J., Feher, V. A., Assa-Munt, N., & Wright, P. E. (1991) *J. Virol. 65*, 1727−1734.
Rance, M., Sørensen, O. W., Bodenhausen, G., Wagner, G., Ernst, R. R., & Wüthrich, K. (1983) *Biochem. Biophys. Res. Commun. 117*, 458−479.
Richardson, J. S., & Richardson, D. C. (1988) *Science 240*, 1648−1652.
Spera, S., & Bax, A. (1991) *J. Am. Chem. Soc. 113*, 5490−5492.
Stott, E. J., & Taylor, G. (1985) *Arch. Virol. 84*, 1−52.
Struthers, M. D., Cheng, R. P., & Imperiali, B. (1996) *Science 271*, 342−345.
Trudel, M., Nadon, F., Séguin, C., & Binz, H. (1991) *Virology 185*, 749−757.
Vriend, G. (1990) *J. Mol. Graphics 8*, 52−56.
Wagner, G., Braun, W., Havel, T. F., Schaumann, T., Go, N., & Wüthrich, K. (1987) *J. Mol. Biol. 196*, 611−639.
Wertz, G. W., Collins, P. L., Huang, Y., Gruber, C., Levine, S., & Ball, L. A. (1985) *Proc. Natl. Acad. Sci. U.S.A. 82*, 4075−4079.
Wishart, D. S., Bigam, C. G., Yao, J., Abildgaard, F., Dyson, H. J., Oldfield, E., Markley, J. C., & Sykes, B. D. (1995) *J. Biomol. NMR 6*, 135−140.
World Health Organization (1995) in *The World Health Report 1995*, WHO, Geneva.
Wüthrich, K. (1986) in *NMR of Proteins and Nucleic Acids*, Wiley Interscience, New York, NY.

BI9621627